II g 3

AN INVESTIGATION OF THE BEARING CAPACITY OF SHALLOW FOOTINGS ON DRY SAND

G.G. MEYERHOF, M.Sc.(Eng.), A.M.I.C.E., AM.I.Struct.E.
Department of Scientific and Industrial Research
Building Research Station

INTRODUCTION.

Although several investigators 1), 2), 3), 4) have carried out small-scale loading tests on sand, their experiments were restricted to surface loads. The bearing capacity of footings and piers located below the surface does not appear to have been determined experimentally, nor is a rigorous analysis of this problem available owing to its mathematical difficulties. In order to assess the value of approximate methods, a preliminary series of model experiments has been made on square and rectangular footings on dry sand, at depths of up to six times the footing width. These tests are briefly described below and the results are analysed on the basis of the observed movements in the sand mass and shear strength of the sand.

METHOD AND RESULTS OF LOADING AND ANCILLARY SHEAR TESTS.

The loading tests were carried out in a stiffened steel tank (Fig. 1) 18 in. long, 15 in. wide and 18 in. deep, which was filled in 3 in. thick layers with a clean and dry medium river sand. The grading lay between 0.3 and 0.6 mm, with 50 per cent. passing a 0.4 mm sieve; the specific gravity of the particles was 2.70. Each layer was tamped with a vibrating hammer, and a fairly uniform density was obtained, the average porosity being 37.1 per cent.

The footings were brass sections ½ and 1 in. wide; their lengths and depths varied from ½ to 6 in. They were placed at the required depth in the centre of the tank and loaded by a jack through a proving ring. The load was applied in small steps, each increment being maintained until the settlement was sensibly complete. The tests were continued beyond the ultimate bearing capacity and the final smallest value until the additional surcharge effect became noticeable and the failure surface was well developed. More information about the extent of the faillure surface was obtained from similar tests on footings in a wooden box with a glass front, the inside face of which had been smoked to record the movement of the soil particles.

The principle results of the loading tests are summarized in Table 1 below.

Some typical tests are illustrated by their settlement-pressure curves in Fig. 2. When a footing was loaded, its settlement increased at an increasing rate until the ultimate bearing capacity was reached. That happened at a settlement of 0.05 to 0.2 times the width of the footing, the lower limit relating to shallower and the upper limit to deeper footings. The final bearing capacity occurred at about twice the above settlement by which time a failure surface usually became noticeable at ground level. With square footings, however, no failure surface was observed for depths greater than twice the footing width.

In plan the failure surface was circular for square and elliptical for rectangular footings, the sand surface rising uniformly for shallow foundation depths (Fig. 3) and as a flat dome for greater depths (Fig. 4). Failure rarely took place with the formation

Arrangement of Loading Test.

FIG.1

of two rupture surfaces, but generally the footing tilted slightly to one side, on which a small crater was produced, with a single failure surface on the other side of the footing (Fig. 5). The corresponding ground movements extended to depths of 2 to 3 times those of the failure surfaces below the foundation base.

The angle of internal friction ϕ of the sand and the angle of skin friction δ of sand on brass were determined in a constant rate of strain shear box 5) for various porosities and vertical pressures. The results (Fig. 6 upper curves) agreed with previous investigations 6), 7) in that although the ultimate (or maximum) (or residual) value ϕ_u increased with smaller porosities and pressures, its final value ϕ_f was independent of them. In the present tests ϕ_f was 30,5°, and the critical porosity varied from 41 per cent. under a normal pressure of ½ t/ft.^{2} to 43½ per cent. under 4 t/ft.^{2}. Similarly the ultimate value δ_u (Fig. 6 lower curves) increased with smaller porosities and pressures, while the final value δ_f was independent and was found to be 18.5°.

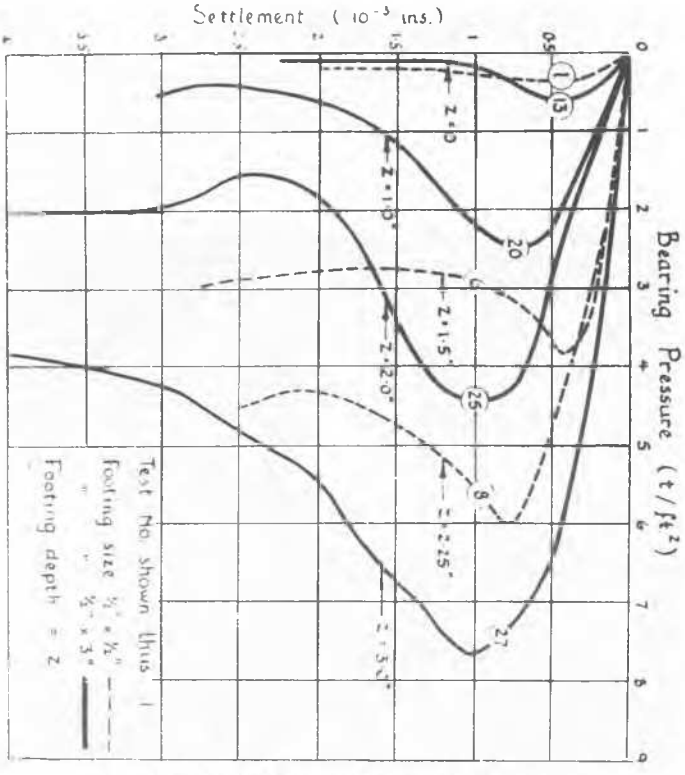

Typical settlement-pressure curves.

FIG.2

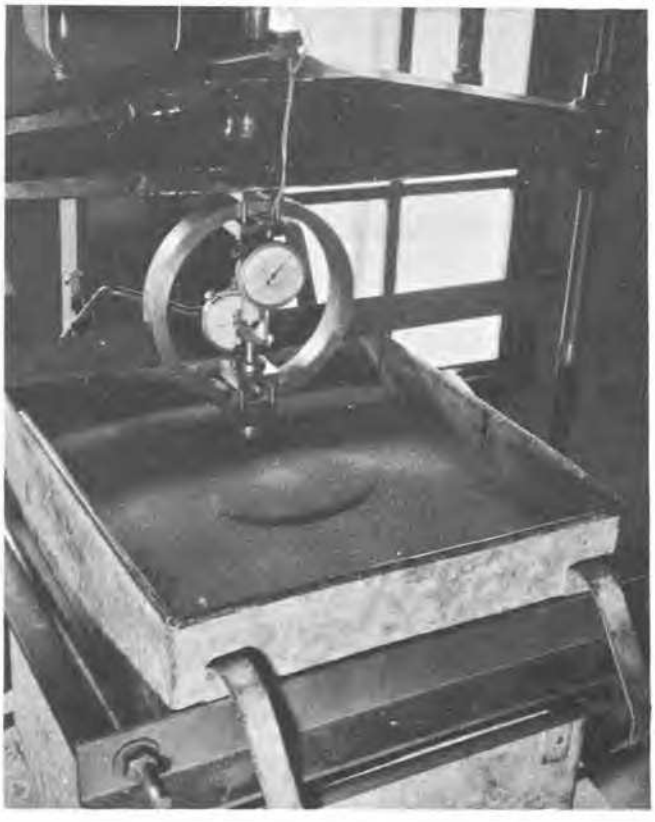

Failure of Footing at Depth equal to Width (Test no. 52).

FIG.3

Failure of Footing at Depth equal to 6 times Width (Test no. 28).

FIG.4

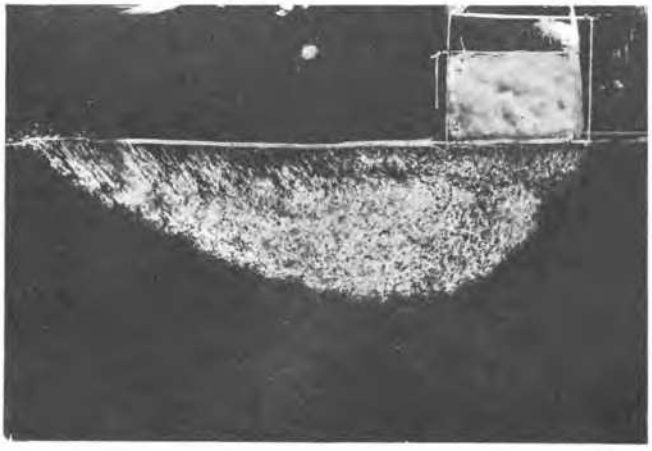

Failure Zone below Surface Footing (Test no. 49).

FIG.5

TABLE 1.

Results of Loading Tests

Test No.	Footing Size	Initial Depth	Average Porosity	Bearing Capacity		Failure Surface	
				Ultimate	Final	Width	Length
		Z	n	q_u	q_f	l_o	
	in.	in.	%	t/ft.^{2}	t/ft.^{2}	in.	in.
1	½ x ½	0	37.0	0.36	0.18	0.5	
2	"	"	37.0	0.39	0.30	0.6	
3	"	"	37.1	0.38	0.35	0.5	
4	"	"	37.1	0.33	0.32	0.5	
5	"	"	36.9	0.35	0.22	0.5	
6	"	1.5	36.5	3.81	2.73	-	
7	"	"	36.5	4.09	2.71	-	
8	"	2.25	36.5	6.0	4.25	-	
9	"	3.03	37.4	6.5	5.3	-	
10	"	3.02	37.3	7.9	6.1	-	
11	½ x 1½	0	37.4	0.35	0.17	1.1	2.2
12	"	"	36.6	0.35	0.22	1.0	1.9
13	½ x 3	"	37.1	0.61	0.10	2.2	3.6
14	"	"	37.0	0.51	0.07	2.1	3.3
15	"	"	37.0	0.46	0.11	1.7	3.2
16	"	"	37.0	0.58	0.26	1.6	3.2
17	"	0.48	36.5	1.52	0.42	3.1	4.2
18	"	0.5	36.9	1.32	0.42	3.2	4.5
19	"	0.9	36.7	2.92	1.54	3.5	5.4
20	"	1.0	36.9	2.52	0.42	4.7	5.8
21	"	1.37	37.3	3.74	0.72	4.8	5.7
22	"	1.42	36.6	3.81	0.65	5.6	7.2
23	"	"	37.1	3.81	0.54	5.2	6.7
24	"	1.95	36.8	4.61	1.51	7.4	6.6
25	"	2.0	36.9	4.41	1.51	6.7	7.6
26	"	2.95	36.8	7.2	2.53	8.0	8.8
27	"	3.0	37.1	7.7	3.29	8.4	9.8
28	"	"	37.0	6.8	2.93	8.2	9.4
29	½ x 4½	0	36.5	0.78	0.20	2.0	5.0
30	"	0.5	36.9	2.01	0.44	3.4	5.3
31	½ x 6	0	36.6	0.48	0.15	2.0	7.0
32	"	"	36.6	0.77	0.14	2.1	6.7
33	"	0.5	36.6	1.87	0.36	3.5	8.0
34	"	0.7	36.8	1.81	0.16	4.8	8.3
35	"	0.88	36.7	2.53	1.34	5.3	8.6
36	1 x 1	0	37.0	0.61	0.46	1.0	
37	"	"	37.8	0.60	0.41	1.1	
38	"	"	37.8	0.60	0.42	1.0	
39	"	"	37.8	0.60	0.41	1.1	
40	"	"	37.8	0.61	0.39	1.0	
41	"	0.8	37.0	2.43	1.38	2.1	
42	"	1.5	38.2	3.68	1.90	3.0	
43	"	"	37.6	3.31	2.41	2.8	
44	"	2.05	36.6	6.7	3.86	3.8	
45	"	3.0	38.3	5.8	4.52	-	
46	"	3.1	37.6	6.8	4.82	-	
47	"	4.45	37.6	8.4	7.5	-	
48	"	6.0	38.1	13.2	12.1	-	
49	1 x 3	0	37.2	1.15	0.23	2.8	4.8
50	"	"	38.0	0.50	0.18	2.6	4.0
51	"	1	36.9	4.15	1.23	7.0	8.2
52	"	"	37.1	3.01	1.17	5.3	6.2
53	"	2	37.5	5.7	1.76	7.6	9.3
54	"	3	37.4	6.6	3.47	11.1	14.7

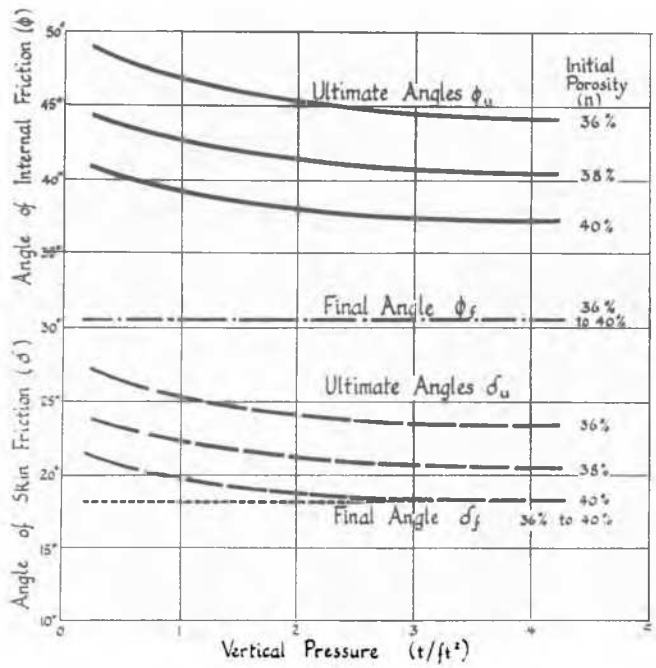

Relation of angles of internal and skin friction and vertical pressure.

FIG.6

In general, $\tan\delta = \frac{1}{2}\tan\phi$ for the same porosity and normal pressure.

ANALYSIS OF RESULTS OF LOADING TESTS.

A comparison by the author 8) of different theories of bearing capacity of shallow foundations indicated that Prandtl's (logarithmic spiral) method 9) was the most promising. Prandtl assumed that the footing edges form the centres of the spiral portions of the failure surface. This assumption does not give the minimum bearing capacity for sands so that such mathematical analyses 10), 11), 12) yield unsafe results. Terzaghi suggested 13) that these centres should be determined by a graphical trial and error method along a line inclined at an angle of $45^\circ - \phi/2$ to the horizontal (Fig.7a) the corresponding analytical determination of the bearing capacity is summarized in the Appendix and leads to a rather involved closed expression from which the coefficients in column 2 of Table 2 have been computed.

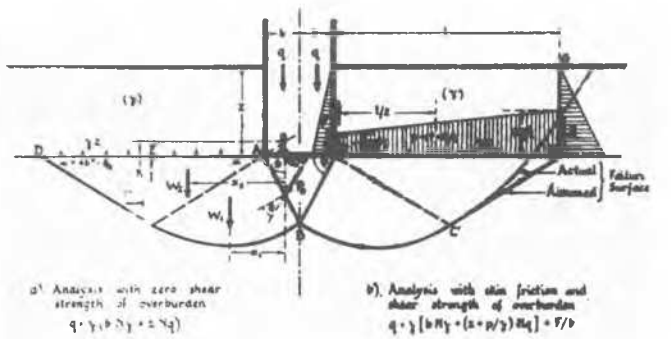

a. Analysis with zero shear strength of overburden. $q = \gamma(b\,N\gamma + z\,Nq)$

b. Analysis with skin friction and shear strength of overburden. $q = \gamma[b\gamma N + (z+p/\gamma)Nq] + F/b$

Analysis of bearing capacity.

FIG.7

The above mentioned values do not, however, represent the worst failure condition, for which the centres of rotation should not be restricted to a line. In this way the lower coefficients in column 3 of Table 2 were obtained together with the width and depth of the failure surfaces. While the difference between the previous and new values is small at low angles of internal friction, it increases rapidly to about 20 per cent. at $\phi = 50^\circ$.

It is somewhat difficult to compare the results of the present tests on surface footings with the theoretical values because ϕ varies with the normal pressure along the failure surface. When an allowance is made for the proportion of the total resistance developed by the various zones of plastic equilibrium, the average normal pressure along the failure surface is of the order of 1/10th of the applied average foundation pressure ($45^\circ < \phi < 46^\circ$) For that pressure (about 0.1 t/ft per inch width of footing) and the average porosity used (37 per cent.), Fig. 6 indicates an average ϕ_u of 46°, giving an ultimate bearing capacity by the modified analysis of $q_{ou} = 0.75$ t/ft. per inch width of footing. This value is in good agreement with the average experimental result of 0.82 t/ft.^{2}. The average observed final bearing capacity $q_{of} = 0.38$ t/ft.^{2} which corresponds to $\phi_f = 42.3^\circ$ is practically the same as that obtained from subsidiary loading tests on the sand in the plastic zone. Although these tests showed that the shearing action occurred

TABLE 2

Theoretical Bearing Capacity and Failure Surface

(Base Angle $\psi = 45^\circ + \phi/2$)

Angle of Internal Friction ϕ	Bearing Capacity Coefficient N_γ		Failure Surface (modified Analysis)	
	Equation 1	Modified Analysis	Width $l_o/2b$	Depth $d_o/2b$
0	0	0	1.0	0.71
5	0.05	0.05	1.1	0.72
10	0.6	0.6	1.2	0.74
15	1.8	1.8	1.4	0.78
20	4.9	4.8	1.7	0.86
25	11.1	10.7	2.2	1.0
30	24.0	22.9	3.0	1.15
35	51.8	48.4	4.1	1.4
40	128	116	4.6	1.7
45	355	305	8.0	2.2
50	1800	1455	12	3.1

throughout that zone, it appeared to be of a partial and progressive nature at different points, as compared with the simultaneous failure along the whole rupture plane in the box shear tests, which gave the much lower Φ_f = 30.5°. The observed maximum depth and width of the failure surface for strip footings were about 2/3rd of the theoretical values for a base angle $\psi = 45° + \Phi/2$. Since in the preliminary tests footings of different roughnesses showed sensibly the same failure surface, the corresponding variation of the base angle suggested by Terzaghi 13) is not supported by this investigation, but the discrepancy must be sought in the theory, which neglects the effect of the weight of the soil on the shape and extent of the failure surface.

The experimental ultimate and average final bearing capacities per unit width of footing are plotted in Fig. 8 against the ratio of depth to width of footing (z/2b). In spite of some scatter of the results, which is largely due to variations in porosity of the sand, the bearing capacities increase in direct proportion with the footing depth within the range investigated. These relations can, with good approximation, be expressed by $q_u = q_{ou} \cdot (1 + 1.4z/b)$ and $q_f = q_{of} \cdot (1 + 1.2z/b)$ for the ultimate and final bearing capacities, respectively. There was a tendency for the ultimate bearing capacities of square footings to be rather less than those of rectangular ones, particularly at ground level where the ratio of the corresponding values was 0.7. The ratio of final to ultimate bearing capacity decreased a little with increasing footing depth and averaged 0.4.

A theoretical estimate of the bearing capacity of shallow footings can be made for the limiting conditions of zero and full shear strength of the sand above foundation level. In the first case a methematical solution (14) (Appendix equation 2) is available from which the ultimate and final bearing capacities are $q_u = q_{ou} \cdot (1 + 0.44z/b)$ and $q_f = q_{of} (1 + 0.49z/b)$ respectively, for $\Phi_u = 45°$ and $\Phi_f = 41.5°$, which would be the upper limits for the higher bearing pressures obtained. These relations have been plotted in Fig. 8 (curves II) and when compared with the test results show that the observed effect of foundation depth is about three times the theoretical one. The shear strenght of the overburden cannot, therefore reasonably be neglected, even for very shallow foundations.

Assuming that the skin friction on the footing and the shear strength along vertical ends of the failure surface are fully mobilized, an approximate analysis can be made on the basis of Terzaghi's method 13) (Appendix equation 3). Preliminary investigation of skin friction in conjunction with the shear test results indicated that nearly the full passive pressure is effective, i.e. $K_0 = K_1 = 5.83$ for $\Phi_u = 45°$ and 4.4 for $\Phi_f = 41.5°$. The distance (ℓ) of the assumed vertical part of the failure surface from the footing edge can be estimated from the observed movements of the sand mass. The experimental ratio of maximum failure surface width (at ground level) to footing width is plotted in Fig. 9 against length/width ratio (a/b) of the footings. These curves show that for a given foundation depth the failure surface width increases with footing length at a decreasing rate, and approaches a maximum for a long strip; for $a/b \geq 6$ this increase appears to be small. Further, Fig. 10, which has been obtained from these curves and Table 1, shows that for a given ratio a/b the failure surface width (ℓ_o) is directly proportional to the footing depth (z), and that for a long strip this relation approximates to $\ell_o = 8b + 3z$. At depths greater than those investigated a maximum ℓ_o seemed to be reached, while later no failure surface at all developed at ground level (e.g. for the deepest square footings tested) owing to the small shear stresses induced there. Since neither depth nor width (ℓ_1) of this surface at base level were appreciably affected by footing depth, i.e. $\ell_1 \doteq 8b$ for a long strip, an average distance $\ell = (\ell_o + \ell_1)/2 = 8b + 1.5z$ may be taken as a rough approximation.

The upper theoretical curves (I) of Fig.8 have been computed from the above results for

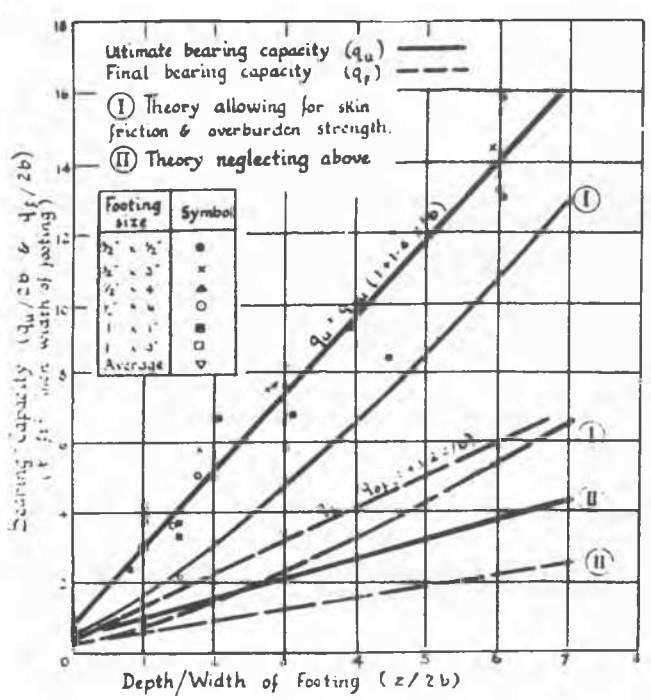

Bearing capacity. Depth relations.

FIG. 8

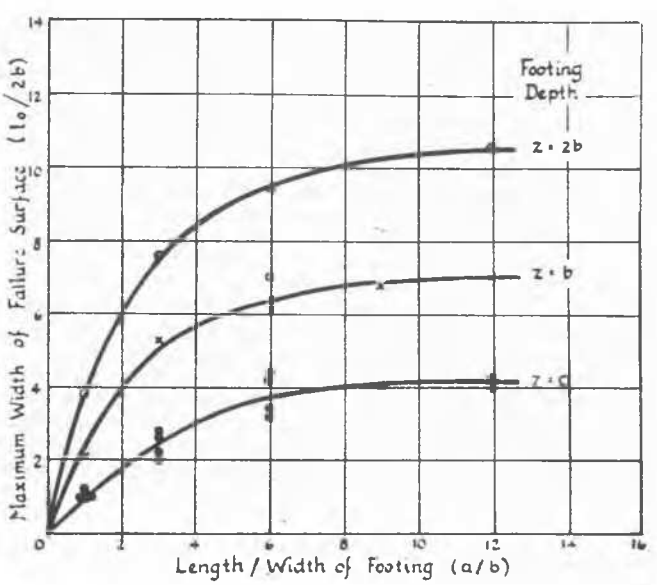

Relation of failure surface width and length of footing.

FIG. 9

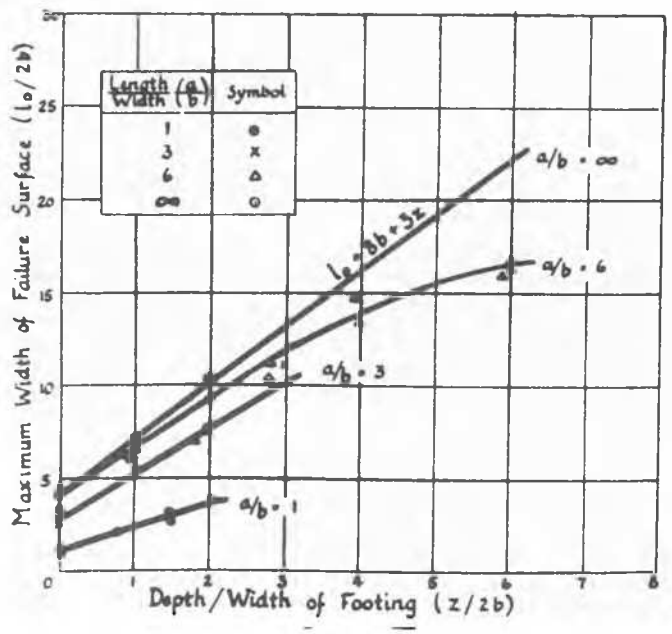

Relation of failure surface width and depth of footing.

FIG.10

the ultimate and final bearing capacities. While the rate of increase of the bearing capacities with footing depth agree closely with that observed in both cases, the estimated values are conservative, particularly for the ultimate condition. This under-estimation may be due to the neglect of greater skin friction and shear resistance near base level caused by the foundation stresses; furthermore, the deformation conditions there might allow the passive pressure ratio to be exceeded locally.

CONCLUSION.

The present model tests show that the ultimate bearing capacity of footings on the surface of dry sand agree fairly well with the theoretical value for the worst failure condition and ultimate shear strenght of the soil.The final bearing capacity is considerably greater than that estimated from the final shear strength, probably owing to partial progressive failure with a limited relative movement of the particles. The width of the failure surface at ground level increases with footing length to a maximum for a long strip when it is less than the value predicted by the modified analysis.

While the bearing capacities of shallow foundations are about three times greater than the values estimated on the assumption of zero shear strength of the overburden, they agree fairly well if the maximum skin friction and full shear strength above base level along a vertical failure plane at the mean observed distance from the footing edge are included. Although the extent of the failure surface varies considerably with bearing areas of different shapes, the corresponding bearing capacities appear to differ mainly for foundations at the surface and at very shallow depths.

ACKNOWLEDGEMENT.

The author is indebted to his colleagues for their assistance in the tests. The work was carried out as part of the programma of the Building Research Baord of the Department of Scientific and Industrial Research, and the paper is published by permission of the Director of Building Research.

BIBLIOGRAPHY.

1) Fellenius, W. "Jordstatiska Beräkningar för vertical Belastning". Teknisk Tidskrift, 1929, Nos. 21 and 25.
2) Kögler F. and A.Scheidig. "Baugrund und Bauwerk". Ernst, Berlin, 1938, p.177.
3) Meischeider, H. "Über den Einfluss der Flächenform auf die Tragfähigkeit von Fundamentplatten". Bauingenieur, 1940, vol.21, p.83
4) Golder, H.Q. "The Ultimate Bearing Pressure of Rectangular Footings". Journ. Inst. C.E., 1941, vol. 17, p.161.
5) Golder, H.Q. "An Apparatus for Measuring the Shear Strength of Soils". Engineering, 1942, vol. 153, p.501.
6) Casagrande, A. and S.G. Albert. "Research on the Shearing Resistance of Soils". Report M.I.T., September 1930.
7) Taylor, D.W. and T.M. Leps. "Shearing Properties of Ottawa Standard Sand". Proc.Soils and Found, Conf., U.S. Corps of Engineers, 1938, p.C-1
8) Meyerhof, G.G. "The Bearing Capacity and Consolidation of Soils and Settlement of Foundations". M.Sc. Thesis, University of London, 1944.
9) Prandtl, L. "Über die Härte plastischer Körper". Nachr.Kgl. Ges. Wiss., Göttingen, Math.-Phys. Kl., 1920, p.74.
10) Palmer, L.A. and E.S.Barber. "Principles of Soil Mechanics Involved in Fill Construction", Proc. Highw.Res. Bd., Washington,1937, vol. 17, p.503.
11) Raes, P.E. "Het Oppersingsvraagstuk bij een Strookvormig Fundament". Techn. - Wetensch. Tijdskr., 1941, No. 10, p.1.
12) Boulton, N.S. "Plastic Stresses in a Semi-Infinite Cohesive Mass". Phil. Mag., 1946, vol. 37, p.733.
13) Terzaghi, K. "Theoretical Soil Mechanics". Wiley, New York, 1940, p.118.
14) Reissner, H. "Zum Erddruckproblem". Proc. 1st.Int.Congr.Appl.Mech., Delft, 1924.

APPENDIX.

Analyses of the Bearing Capacity of a Strip Footing on Sand.

1) Load at Ground Level (Fig. 7a with z = 0)

When the bearing capacity is q, the plastic equilibrium to the left of the footing centre is found by balancing the moments about O (on CA produced and defined by angle θ between CO and the vertical) of the overturning resultant Po on AB and the resisting sector ABC (force W_1) and wedges ACE (W_2) and CDE (P_1).

Thus $$M_0 = M_1 + M_2 + M_3$$

where $M_0 = P_0 x_0$, $M_1 = W_1 x_1$, $M_2 = W_2 x_2$ and $M_3 = P_1 y_1$

Omitting details of the analysis and using the notation illustrated in Fig. 7, it can be shown that

$$M_0 = \frac{(2q+\gamma v \tan\psi)v^2 \tan\psi}{2\cos(\psi-\phi)}\left[\frac{2\cos\phi}{3\sin\psi} - \frac{(\cot\psi - \tan\theta)\cos(\alpha+\psi-\phi)}{(\cot\alpha+\tan\theta)\sin\alpha}\right],$$

$$M_1 = M_1' - M_1'', \text{ where}$$

$$M_1' = \frac{\gamma v^3 \tan^3\psi(\cot\alpha+\cot\psi)^3}{3(\cot\alpha+\tan\theta)^3\cos^3\theta(9\tan^2\Phi+1)}\left[(3\tan\Phi\cos\alpha-\sin\alpha)e^{3(45°+\Phi/2+\theta)\tan\Phi}\right.$$
$$\left. +3\tan\Phi\sin\theta+\cos\theta\right] \quad \text{and}$$

$$M_1'' = \frac{\gamma v\tan^2\psi(\cot\psi-\tan\theta)(1+\tan\psi\cot\alpha)}{3(\cot\alpha+\tan\theta)}\left[\frac{(\cot\psi-\tan\theta)\cot\alpha}{\cot\alpha+\tan\theta} - \frac{\cot\psi}{2}\right],$$

and $M_2 = M_3$

$$= \frac{\gamma v^3\tan^3\psi}{6}\left[(A-B)^2\cot^2\alpha(2A+B)\right]$$

where $A = \dfrac{\cos\alpha+\sin\alpha\cot\psi}{(\cot\alpha+\tan\theta)\cos\theta}e^{(45°+\Phi/2+\theta)\tan\Phi}$

and $B = \dfrac{\cot\psi-\tan\theta}{\cot\alpha+\tan\theta}$

Substituting the above into the equilibrium equation and simplifying,

$$q = \gamma v N_\gamma \qquad (1)$$

where $N_\gamma = \dfrac{\tan\psi}{3}[C]$ the expansion of C being

$$\left[\frac{\tan\psi}{(\cot\alpha+\tan\theta)^3}\left\{\left(\frac{\cos\alpha+\sin\alpha\cot\psi}{\cos\theta}e^{(45°+\Phi/2+\theta)\tan\Phi}-\cot\psi+\tan\theta\right)^2\cdot\right.\right.$$
$$\left.\left.\cdot\left(\frac{\cos\alpha+\sin\alpha\cot\psi}{\cos\theta}2e^{(45°+\Phi/2+\theta)\tan\Phi}+\cot\psi-\tan\theta\right)\cot^2\alpha\right\}\right]$$
$$+\frac{\tan\psi}{(\cot\alpha+\tan\theta)^3}\left\{\frac{(\cot\alpha+\cot\psi)^3}{(9\tan^2\Phi+1)\cos^3\theta}\left(e^{3(45°+\Phi/2+\theta)\tan\Phi}[3\tan\Phi\cos\alpha-\sin\alpha]\right.\right.$$
$$\left.\left.+3\tan\Phi\sin\theta+\cos\theta\right)\right\}$$
$$-\frac{1}{(\cot\alpha+\tan\theta)^2}\left\{(\cot\psi-\tan\theta)\left[\left(\frac{\cot\psi}{2}-\tan\theta\right)\cot\alpha-\frac{\cot\psi}{2}\tan\theta\right](1+\tan\psi\cot\alpha)\right\}$$
$$\left\{\frac{2\cos\Phi}{3\sin\psi}-\frac{\cos(\alpha+\psi-\Phi)}{\sin\alpha}\left(\frac{\cot\psi-\tan\theta}{\cot\alpha+\tan\theta}\right)\right\}\div\cos(\psi-\Phi)\Bigg]^{3/2}$$

The worst θ is found by solving $dN_\gamma/d\theta = 0$, which has been done for two special cases:-

1) $\psi = 45° + \dfrac{\Phi}{2}$ when $\theta \simeq \dfrac{4\alpha}{3} = 60° - \dfrac{2\Phi}{3}$

and 2) $\psi = \Phi$ when $\theta \simeq \dfrac{2\alpha}{5} = 18° - \dfrac{\Phi}{5}$

By substituting either of these equations into the general equation of the bearing capacity above, it can be simplified a little.

2) Load at Depth z below Ground Level

a) Zero shear strength of overburden (Fig. 7a)

$$q = \gamma(vN_\gamma + zN_q) \qquad (2)$$

where 14) $N_q = \dfrac{\cos(\psi-\Phi)}{\cos\psi\tan\alpha}e^{(270°+\Phi-2\psi)\tan\Phi}$

$$\therefore N_q = \cot^2\alpha\, e^{180°\tan\Phi} \qquad \text{for } \psi = 45° + \frac{\Phi}{2}$$

and $$= \frac{\cot\alpha}{\cos\Phi}e^{(270°-\Phi)\tan\Phi} \qquad \text{for } \psi = \Phi$$

b) Full skin friction and shear strength of overburden (Fig. 7b)

The bearing capacity is increased from the value of equation (2) by the skin friction F on the footing and the average surcharge pressure p due to F and the shear strength S along the vertical part D'G of the failure surface.

Hence $$q = \gamma\left[vN_\gamma + \left(z+\frac{p}{\gamma}\right)N_q\right] + \frac{F}{b} \qquad (3)$$

where
$F = K_o\tan\delta\,\frac{1}{2}\gamma z^2$
$S = K_1\tan\Phi\,\frac{1}{2}\gamma z^2$
$p = \dfrac{F+S}{\ell}$
K_o and K_1 are the earth pressure coefficients at the footing side and vertical part of the failure surface, respectively.

-o-o-o-o-o-o-